Electronic Supplementary Information

“Cooking” Hierarchically Porous Carbons with Phenolic Molecules and Zinc Salts

Le-Le Zhang,[a‡] Lei Tong,[a‡] Yan-Wei Ding,[a] Lin-Wei Chen,[a] Yu-Xia Bai,[a] Lv-Dan Liu,[a] and Hai-Wei Liang[a*]

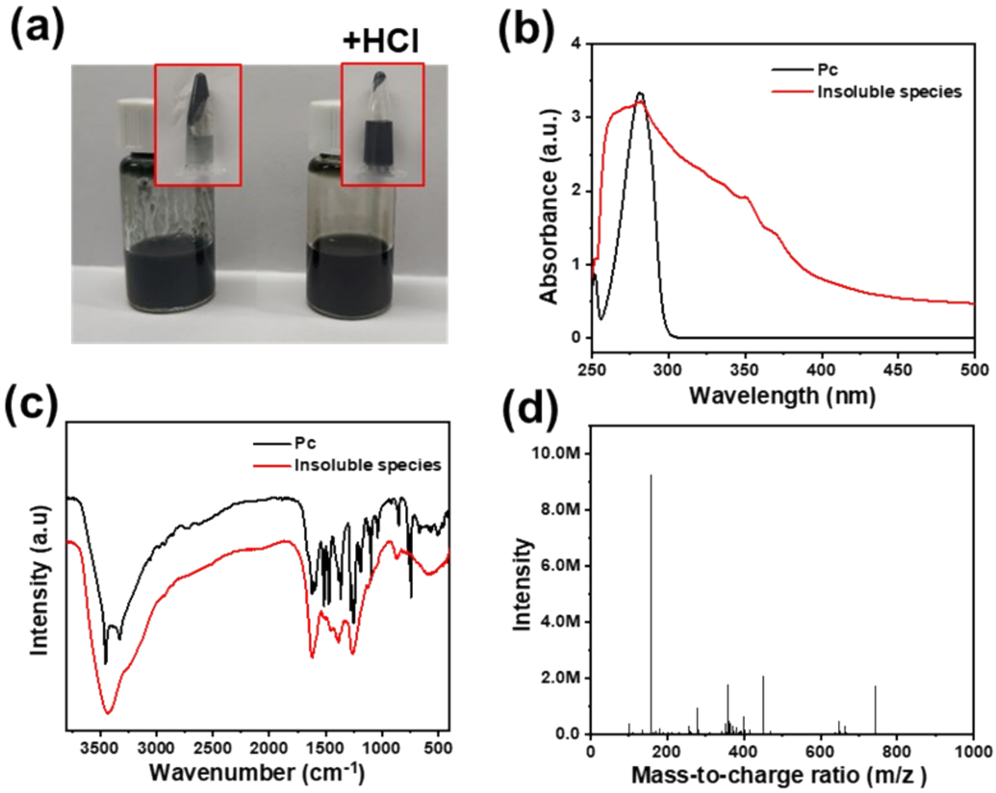

Figure S1. (a) UV-Vis and (b) FT-IR spectra of Pc and insoluble species. (c) ESI-MS spectra of insoluble species. The presence of a large, broad absorption tail for insoluble species spectrum from 300-500 nm, indicates an extended degree of conjugation of π-bonds in the polymer[1-3]. FT-IR spectra also manifested the presence of oligomer, as evidenced by the disappearance of four absorption peaks characteristic of the benzene ring when compared with Pc[3-5]. Further evidence in the mass spectrums showed the presence of oligomeric species.

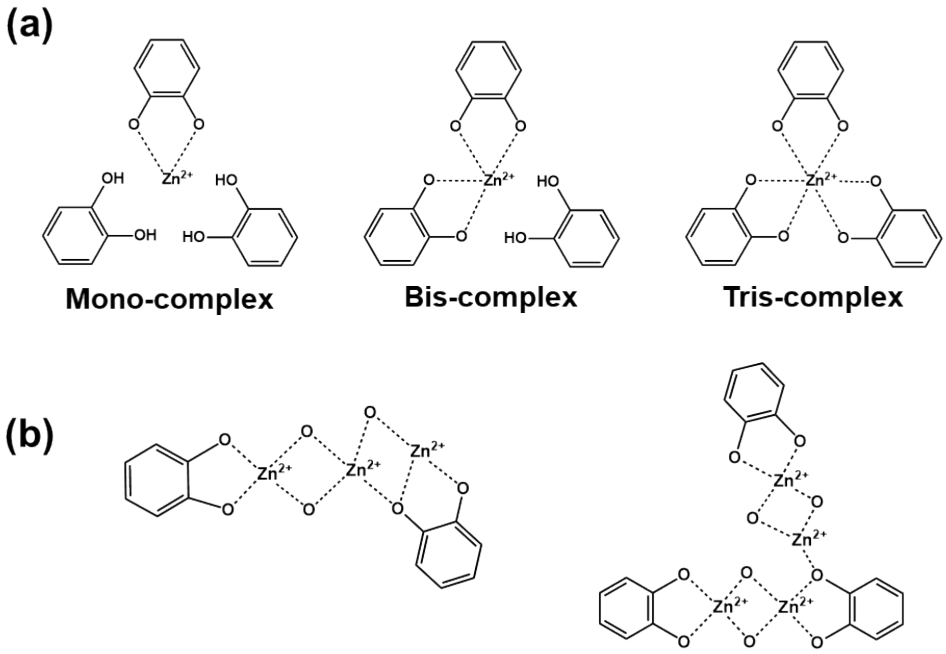

Figure S2. (a) Typical complexation states of Pc. (b) Hypothetical coordination mode for the vicinal di-hydroxyl group of Pc in the resulting PcZn complex.

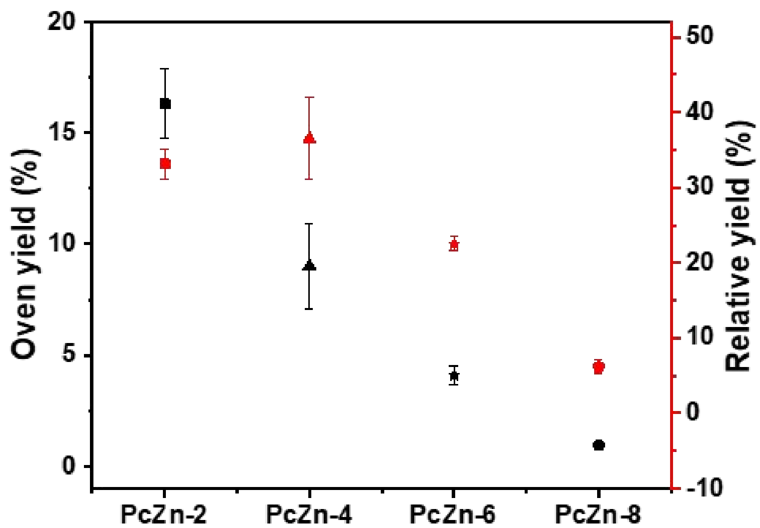

Figure S3. Oven yield and relative yield of PcZn. Note: Relative carbon yield refers to the ratio between oven yield and theoretical yield; theoretical yield was calculated based on the overall carbon contents in the molecule used.

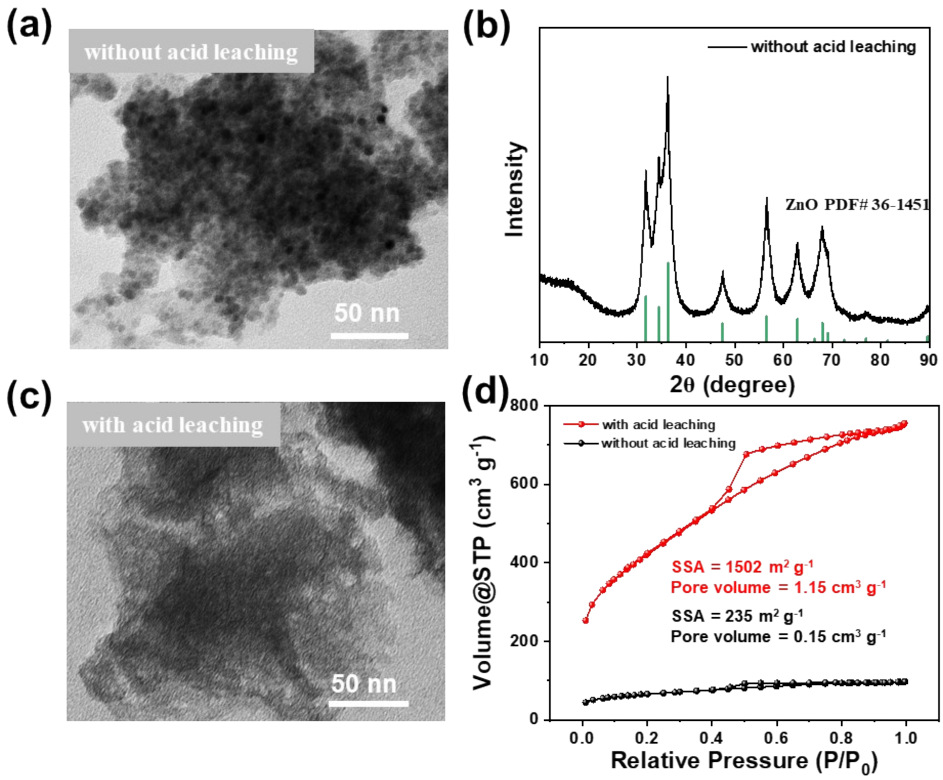

Figure S4. TEM images, XRD patterns and nitrogen sorption isotherms of sample obtained by pyrolysis of PcZn-4 at 600 °C with and without acid leaching.

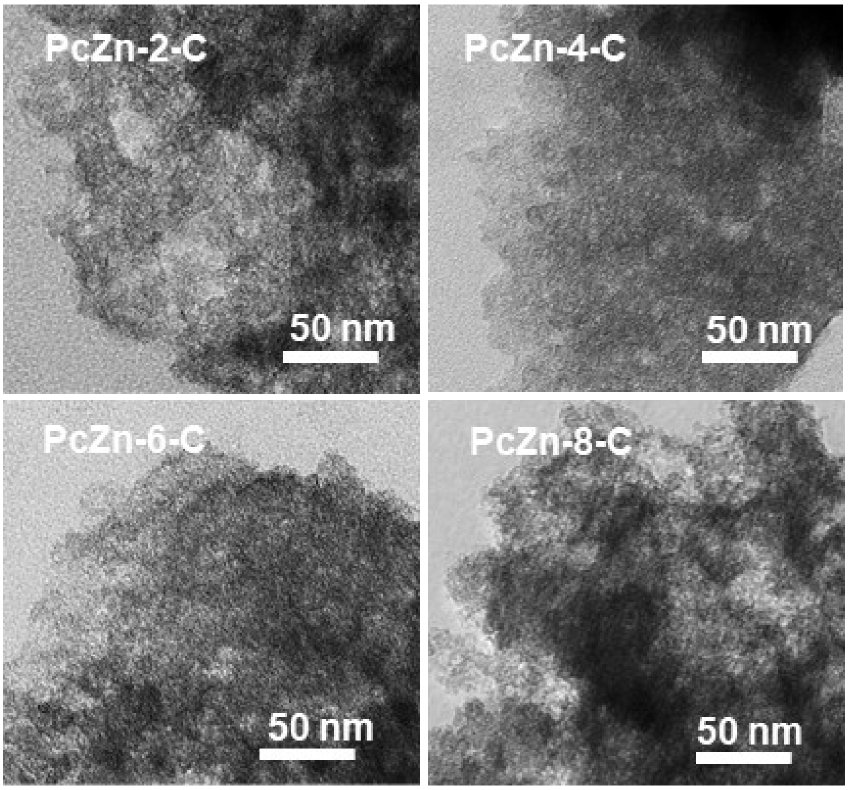

Figure S5. TEM images of the HPCs synthesized by different phenolic molecules

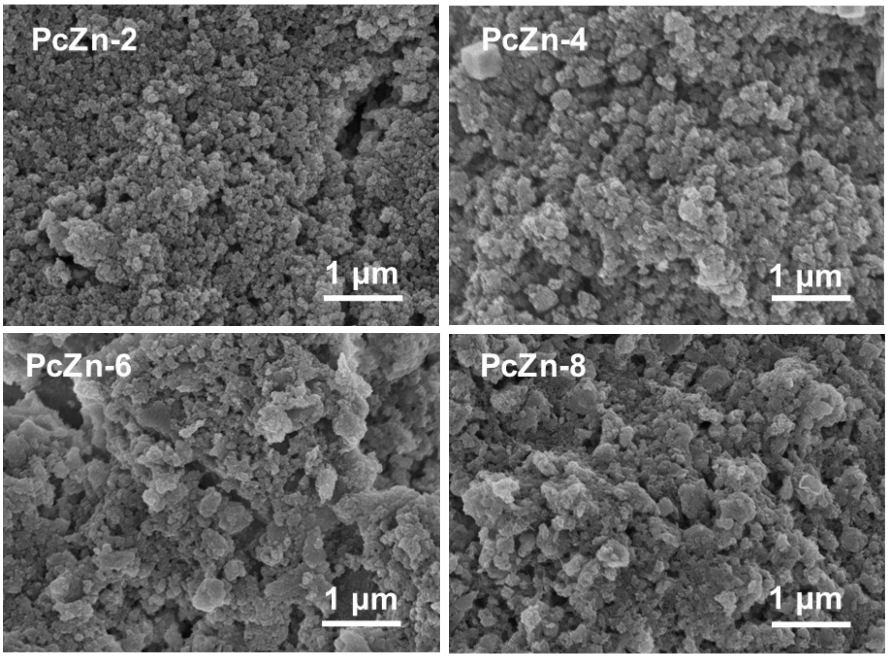

Figure S6. SEM images of metal complexing compounds.

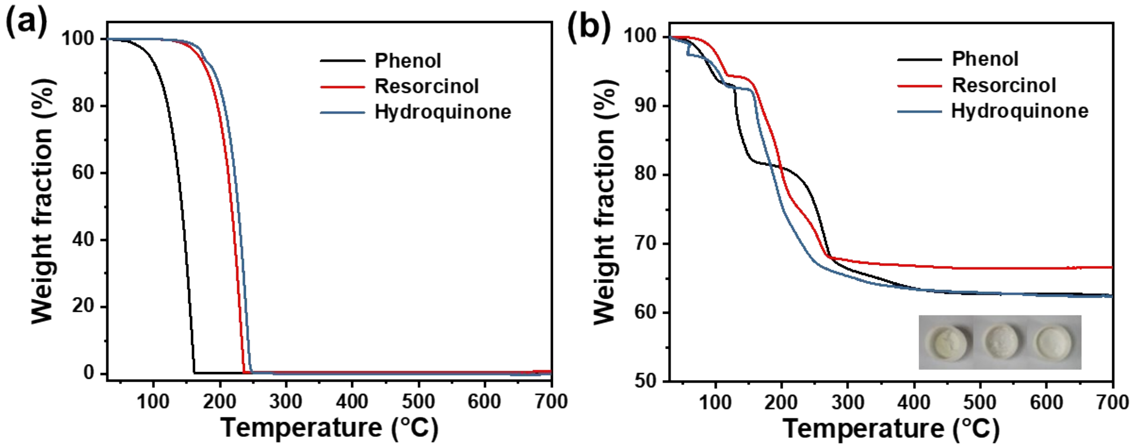

Figure S7. TGA curves of ligands (a) and molecule metal-ligand compounds (b) made by coordinating Zn^{2+} with phenol, resorcinol, and hydroquinone in N_2 atmosphere.

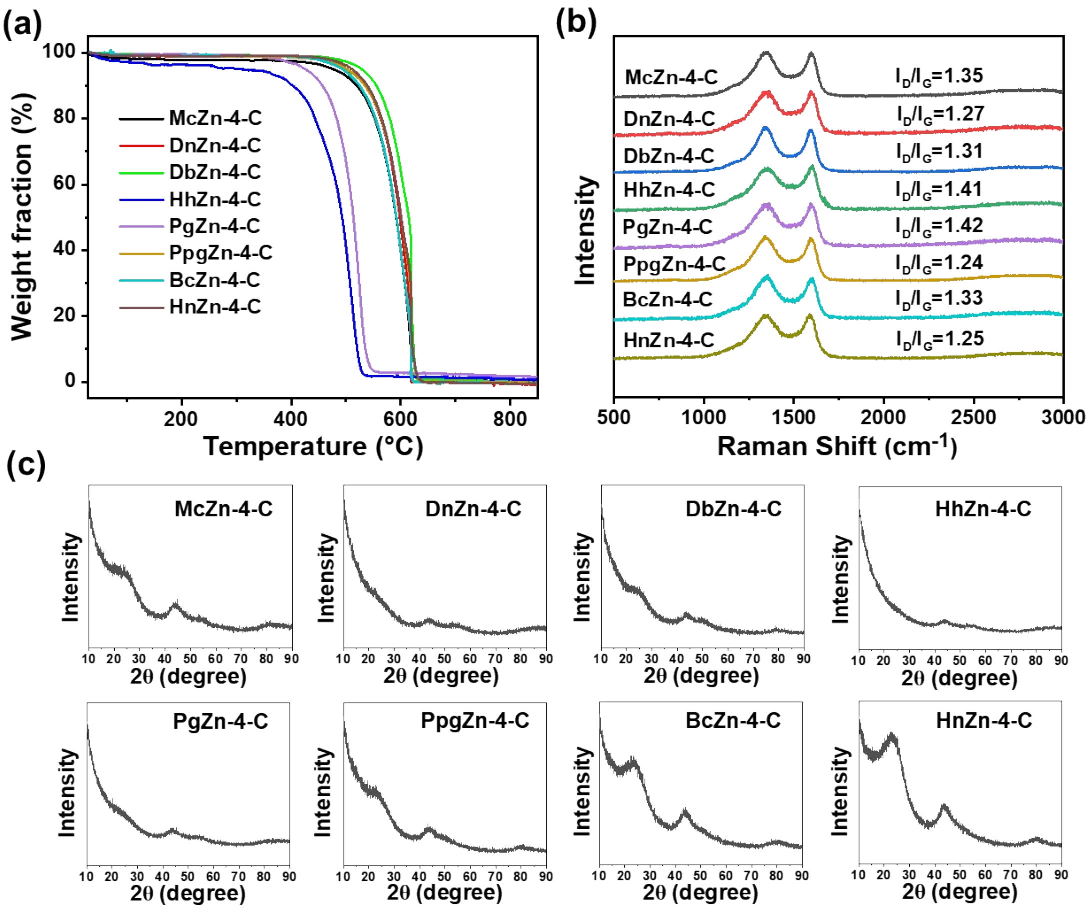

Figure S8. TGA curves in air atmosphere (a), Raman spectra (b) and XRD patterns (c) of the HPCs synthesized from different phenolic molecules.

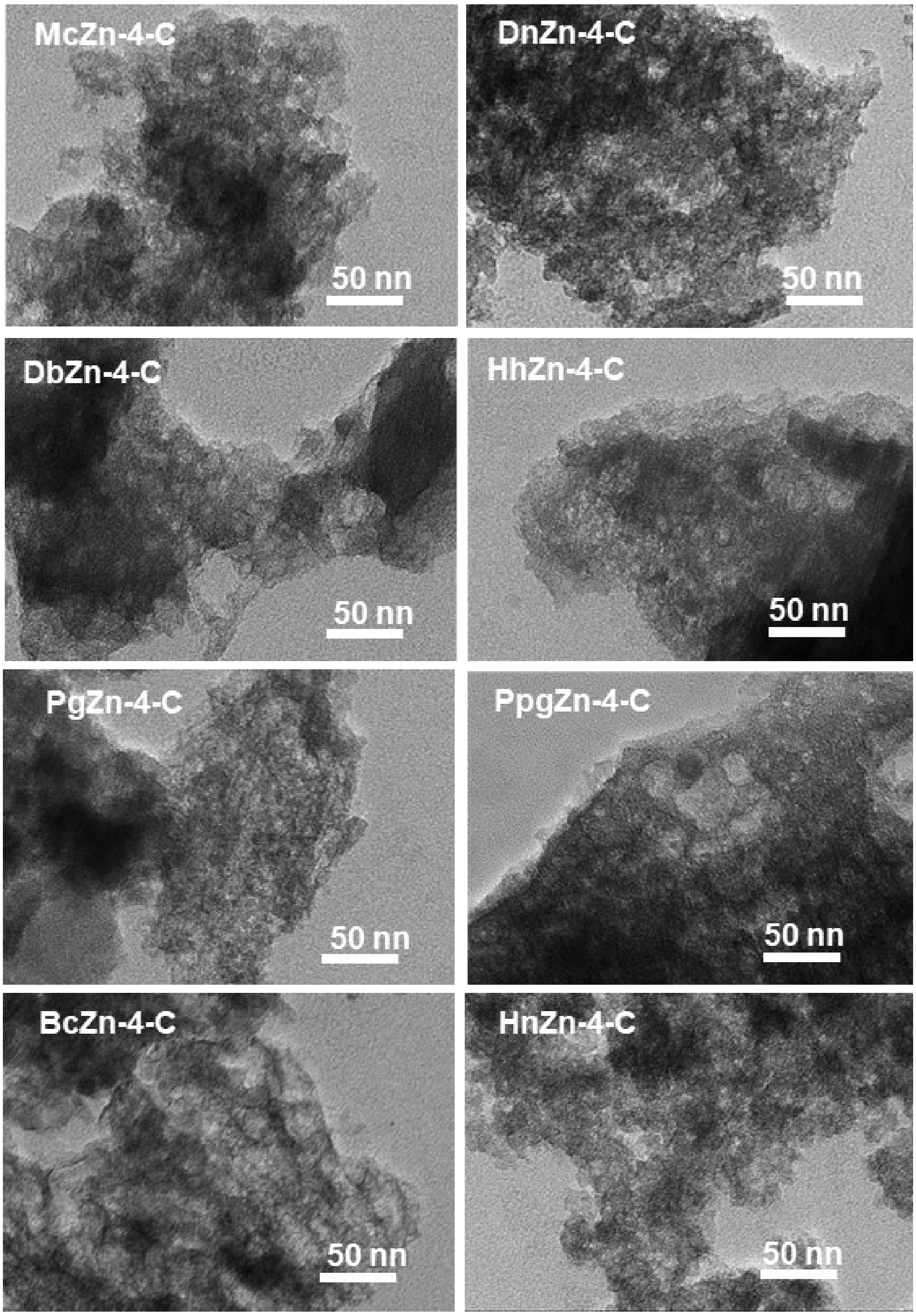

Figure S9. TEM images of the HPCs synthesized by different phenolic molecules.

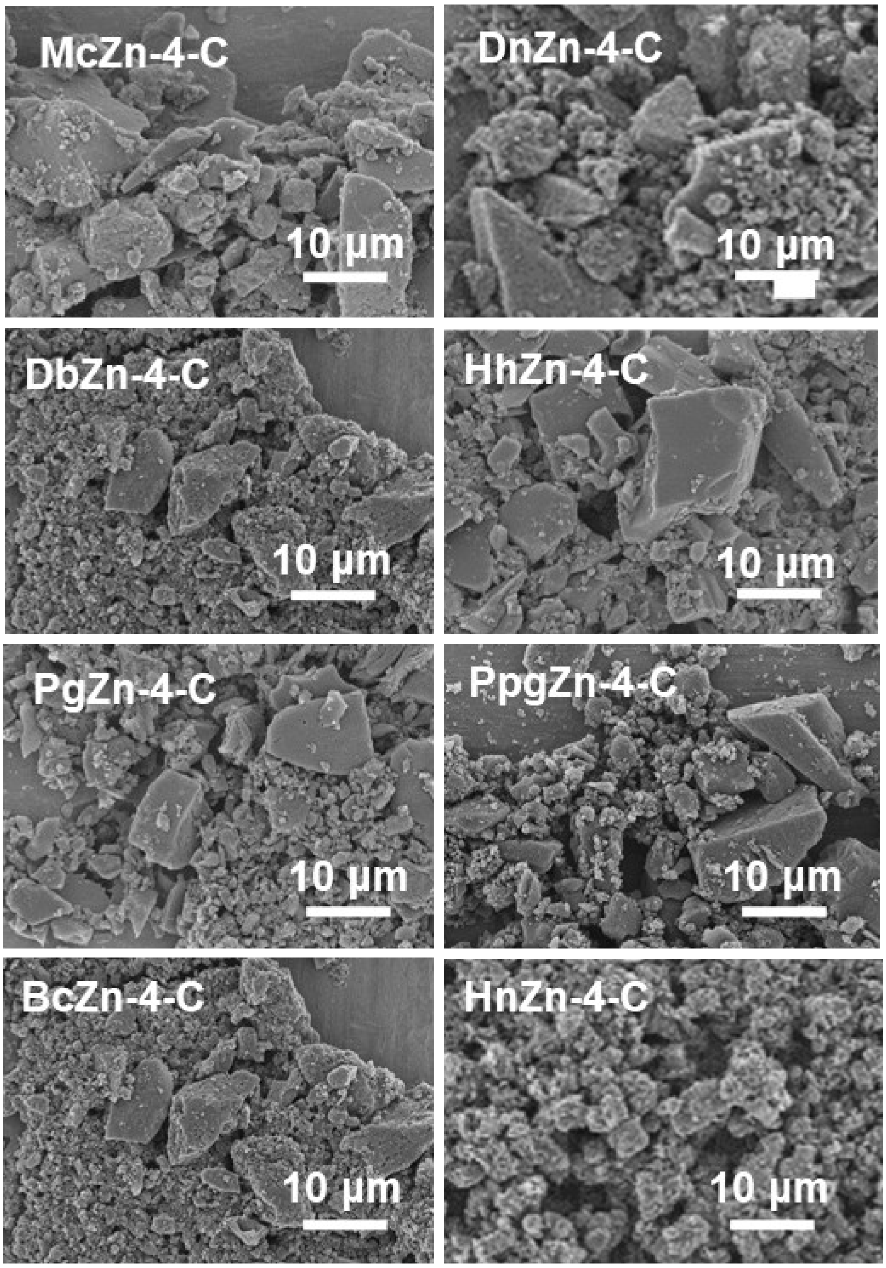

Figure S10. SEM images of the HPCs synthesized from different phenolic molecules.

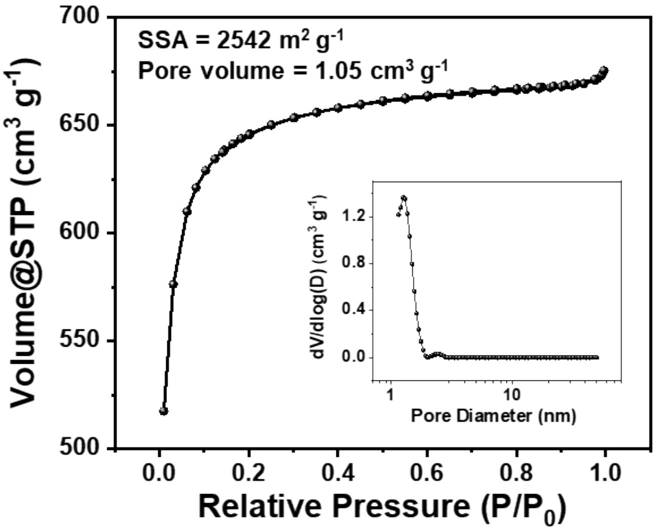

Figure S11. Nitrogen sorption isotherm and pore size distribution of KOH-C.

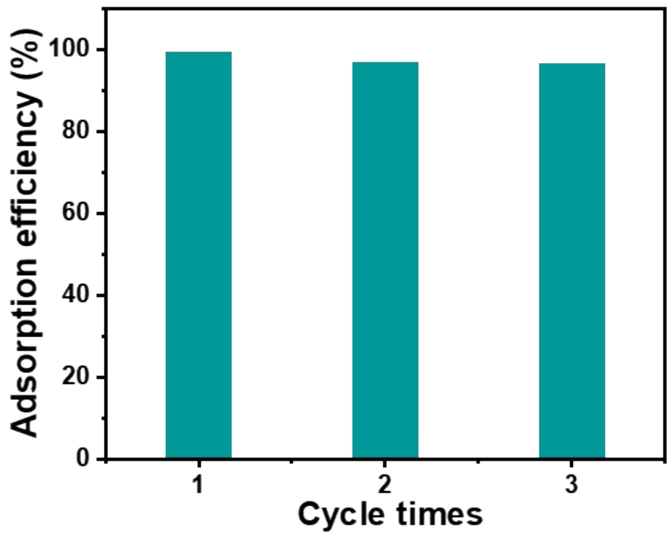

Figure S12. Adsorption efficiency of RhB onto PcZn-8-C in three successive cycles.

Table S1. Textural characteristics of the as-prepared HPCs.

Molecules	SSAs (m^2 g^{-1})	Total pore volume (cm^3 g^{-1})	Micropore volume (cm^3 g^{-1})	Mesopore volume (cm^3 g^{-1})
PcZn-2-C	1720	1.42	0.45	0.83
PcZn-4-C	2043	1.81	0.43	1.22
PcZn-6-C	2322	2.21	0.49	1.49
PcZn-8-C	2753	3.36	0.62	1.92
McZn-4-C	1392	1.11	0.38	0.62
DnZn-4-C	1655	1.48	0.43	0.93
DbZn-4-C	1355	1.00	0.45	1.24
HhZn-4-C	1460	1.18	0.40	0.70
PgZn-4-C	2180	1.80	0.61	0.96
PpgZn-4-C	1355	0.99	0.38	0.54
BcZn-4-C	1000	0.70	0.32	0.30
HnZn-4-C	1188	0.78	0.33	0.30
KOH-C	2542	1.05	0.95	0

Table S2. Pseudo-first-order and pseudo-second-order rate constants for RhB adsorption on PcZn-8-C and KOH-C.

Parameter	Pseudo-first-order			Pseudo-second-order		
	k_1 (min^{-1})	q_e (mg g^{-1})	R_1^2	k_2 ($\times10^{-3}$ g mg^{-1} min^{-1})	q_e (mg g^{-1})	R_2^2
PcZn-8-C	0.27	13.1	0.534	21.0	203	0.999
KOH-C	0.019	113	0.920	0.53	205	0.998

Table S3. Parameters of Langmuir and Freundlich isotherms for RhB adsorption on HPCs and KOH-C.

Adsorbent	Langmuir model			Freundlich model		
	q_{max} (mg g^{-1})	K_L (mg g^{-1})	R_1^2	K_F (mg g^{-1})	n^{-1}	R_2^2
PcZn-8-C	1251	7.27	0.997	1052	0.034	0.840
KOH-C	238	3.65	0.997	146	0.094	0.775

Table S4. Comparison of RhB adsorption capacities of different adsorbent materials.

Absorbent	SSAs ($m^2\ g^{-1}$)	Total pore volume ($m^3\ g^{-1}$)	Adsorption capacity ($mg\ g^{-1}$)	reference
Rice husk based porous carbon	1886	0.98	489	6
Porous carbon nanosphere	2902	1.49	1409	7
Mesoporous carbon fiber	2092	1.37	469	8
Ordered mesoporous carbon	1906	1.8	1028	9
Mesoporous activated carbon	1947	1.71	714	10
Boron nitride foam-like porous monolith	1406	0.89	554	11
Hollow porous organic polymer	869	0.46	460	12
Nickel and carbon hybrids	999	0.86	395	13
Nitrogen-doped porous carbon	3376	1.66	704	14
Porous anionic hyper cross linked polymer	939	1.12	230	15
Porous organic copolymer	848	0.78	422	16
Hyper-cross-linked resins	1066	0.77	394	17
ZIF-8	1285	0.61	25	18
Porous borocarbonitride nanosheet	861	2.5	301	19
N-doped mesoporous gyroid carbon	539	0.69	204	20
Ordered mesoporous carbons	2426	2.17	265	21
Covalent triazine framework	2071	1.33	484	22
HPCs	**2753**	**3.36**	**1251**	**This work**

References

1. R. M. Duarte, E. B. Santos and A. C. Duarte, Spectroscopic characteristics of ultrafiltration fractions of fulvic and humic acids isolated from an eucalyptus bleached Kraft pulp mill effluent, *Water Res.*, 2003, **37**, 4073-4080.
2. F. F. Bruno, J. A. Akkara, L. A. Samuelson, D. L. Kaplan, B. K. Mandal, K. A. Marx, J. Kumar and S. K. Tripathy, Enzymic Mediated Synthesis of Conjugated Polymers at the Langmuir Trough Air-Water Interface, *Langmuir*, 1995, **11**, 889-892.
3. F. F. Bruno, R. Nagarajan, P. Stenhouse, K. Yang, J. Kumar, S. K. Tripathy and L. A. Samuelson, Polymerization of water-soluble conductive polyphenol using horseradish peroxidase, *J. Macromol. Sci. A*, 2001, **38**, 1417-1426.
4. P. K. Jha and G. P. Halada, The catalytic role of uranyl in formation of polycatechol complexes, *Chem. Cent. J.*, 2011, **5**, 1-7.
5. N. Aktaş, N. Şahiner, Ö. Kantoğlu, B. Salih and A. Tanyolaç, Biosynthesis and characterization of laccase catalyzed poly (catechol), *J. Polym. Environ.*, 2003, **11**, 123-128.
6. Y. P. Guo, J. Z. Zhao, H. Zhang, S. F. Yang, J. R. Qi, Z. C. Wang and H. D. Xu, Use of rice husk-based porous carbon for adsorption of Rhodamine B from aqueous solutions, *Dyes Pigm.*, 2005, **66**, 123-128.
7. B. Chang, D. Guan, Y. Tian, Z. Yang and X. Dong, Convenient synthesis of porous carbon nanospheres with tunable pore structure and excellent adsorption capacity, *J. Hazard. Mater.*, 2013, **262**, 256-264.
8. Y. Dong, H. Lin, Q. Jin, L. Li, D. Wang, D. Zhou and F. Qu, Synthesis of mesoporous carbon fibers with a high adsorption capacity for bulky dye molecules, *J. Mater. Chem. A*, 2013, **1**, 7391-7398.
9. P. K. Tripathi, M. Liu, L. Gan, J. Qian, Z. Xu, D. Zhu and N. N. Rao, High surface area ordered mesoporous carbon for high-level removal of rhodamine B, *J. Mater. Sci.*, 2013, **48**, 8003-8013.
10. A. Jain, R. Balasubramanian and M. P. Srinivasan, Production of high surface area mesoporous activated carbons from waste biomass using hydrogen peroxide-mediated hydrothermal treatment for adsorption applications, *Chem. Eng. J.*, 2015, **273**, 622-629.
11. Y. Xue, P. Dai, X. Jiang, X. Wang, C. Zhang, D. Tang, Q. Weng, X. Wang, A. Pakdel, C. Tang, Y. Bando and D. Golberg, Template-free synthesis of boron nitride foam-like porous monoliths and their high-end applications in water purification, *J. Mater. Chem. A*, 2016, **4**, 1469-1478.
12. H.-J. Zhang, J.-H. Wang, Y.-H. Zhang and T.-L. Hu, Hollow Porous Organic Polymer: High-Performance Adsorption for Organic Dye in Aqueous Solution, *J. Polym. Sci. Pol. Chem.*, 2017, **55**, 1329-1337.
13. L. Jin, X. Zhao, X. Qian and M. Dong, Nickel nanoparticles encapsulated in porous carbon and carbon nanotube hybrids from bimetallic metal-organic-frameworks for highly efficient adsorption of dyes, *J. Colloid Interface Sci.*, 2018, **509**, 245-253.
14. L. Lv, Y. Huang and D. Cao, Nitrogen-doped porous carbons with ultrahigh specific surface area as bifunctional materials for dye removal of wastewater and supercapacitors, *Appl. Surf. Sci.*, 2018, **456**, 184-194.
15. R. Shen, X. Yan, Y.-J. Guan, W. Zhu, T. Li, X.-G. Liu, Y. Li and Z.-G. Gu, One-pot synthesis of a highly porous anionic hypercrosslinked polymer for ultrafast adsorption of organic pollutants, *Polym. Chem.*, 2018, **9**, 4724-4732.
16. T. Xu, Y. He, Y. Qin, C. Zhao, C. Peng, J. Hu and H. Liu, Facile preparation of porous organic copolymer based on triptycene and crown ether for efficient organic dye adsorption, *RSC Adv.*, 2018, **8**, 4963-4968.
17. T. Zhang, F. Zhou, J. Huang and R. Man, Ethylene glycol dimethacrylate modified hyper-cross-linked resins: Porogen effect on pore structure and adsorption performance, *Chem. Eng. J.*, 2018, **339**, 278-287.
18. T. Ba Luan, H.-Y. Chin, B. K. Chang and A. S. T. Chiang, Dye adsorption in ZIF-8: The importance of external surface area, *Microporous Mesoporous Mater.*, 2019, **277**, 149-153.

19. Q. Hao, Y. Song, Z. Mo, S. Mishra, J. Pang, Y. Liu, J. Lian, J. Wu, S. Yuan, H. Xu and H. Li, Highly Efficient Adsorption of Oils and Pollutants by Porous Ultrathin Oxygen-Modified BCN Nanosheets, *ACS Sustain. Chem. Eng.*, 2019, **7**, 3234-3242.
20. A. F. M. El-Mahdy, T.-E. Liu and S.-W. Kuo, Direct synthesis of nitrogen-doped mesoporous carbons from triazine-functionalized resol for CO2 uptake and highly efficient removal of dyes, *J. Hazard. Mater.*, 2020, **391**, 122163.
21. T. Shi, Y. Wen, C. Ma, S. Jia, Z. Wang and S. Zou, Adsorption Characteristics of Phenol and Reactive Dyes from Aqueous Solution onto Ordered Mesoporous Carbons Prepared via a Template Synthesis Route, *Adsorpt. Sci. Technol.*, 2009, **27**, 643-659.
22. T. Wang, K. Kailasam, P. Xiao, G. Chen, L. Chen, L. Wang, J. Li and J. Zhu, Adsorption removal of organic dyes on covalent triazine framework (CTF), *Microporous Mesoporous Mater.*, 2014, **187**, 63-70.